

EXPLORATION OF LOW-ASPECT-RATIO TOKAMAK REGIMES IN THE CDX-U AND TS-3 DEVICES

Y.S. HWANG, M. YAMADA, T.G. JONES, M. ONO, W. CHOE,
S.C. JARDIN, E. LO, G. LUDWIG¹, J. MENARD, Å. FREDRIKSEN²,
R. NAZIKIAN, N. POMPHREY, S. YOSHIKAWA
Plasma Physics Laboratory,
Princeton University,
Princeton, New Jersey,
United States of America

A. MORITA, Y. ONO, T. ITAGAKI, M. KATSURAI, K. TOKIMATSU
Department of Electrical Engineering,
University of Tokyo,
Tokyo, Japan

Abstract

EXPLORATION OF LOW-ASPECT-RATIO TOKAMAK REGIMES IN THE CDX-U AND TS-3 DEVICES.

In the low-aspect-ratio tokamak regime, a lower $q(a)$ regime (i.e. $q(a) \leq 5$, $A = R/a \approx 1.5$) has been explored in CDX-U, and the ultra-low-aspect-ratio tokamak regime ($1.05 \leq A \leq 1.5$) has been explored in TS-3. Using a relatively low toroidal magnetic field, plasma discharges with $I_p \leq 53$ kA and $q(a) \geq 4$ [$q_{cy1}(a) \geq 1$] have been obtained in CDX-U. Low $q(a)$, ohmic plasmas in CDX-U show increasing MHD activity as the edge safety factor is lowered. These modes appear to reduce the current ramp-up rate and, at present, limit the access to even lower $q(a)$ regimes. An experiment carried out in the ULART regime ($A \approx 1.05 - 1.5$) on the TS-3 device identifies a threshold of $q(a) \geq 3$ with $q_{cy1}(a) < 1$ for stability of global tilt/shift modes.

1. Introduction

The low-aspect-ratio tokamak (LART) and ultra-low-aspect-ratio (ULART) tokamak configurations offer interesting possibilities for a cost-effective, high-performance (high stable beta in the first stability boundary) plasma regime which lend themselves naturally to a compact volumetric neutron source as well as a high beta advanced fuel reactor [1]. The recent results from START have been encouraging [2]. Non-inductive current drive results using internally generated bootstrap currents and helicity injection current drive in a low-aspect-ratio configuration have been reported previously [3]. To extend the parameter range of the low-aspect-ratio tokamak regime, a new class of 1 MA level devices is being considered (e.g., NSTX [4]). The CDX-U tokamak at

¹ Instituto Nacional de Pesquisas Espaciais, São Paulo, Brazil.

² University of Tromsø, Tromsø, Norway.

Princeton [3] with the recent installation of an ohmic solenoid can be used to proto-type LARTs such as NSTX. In a typical LART design, due to the limited ohmic heating coil capability, an efficient tokamak start-up assist would be particularly important for saving valuable ohmic volt-seconds. Among various LART regimes, it is important to explore a lower $q(a)$ regime [i.e. $q(a) \leq 5$] since the MHD [5] and kinetic mode stabilities [6] are expected to change with $q(a)$ and $A = R/a$.

The ULART configuration, $A \leq 1.4$, is similar to the spheromak in its strong paramagnetism and magnetic helical pitch. As the aspect ratio and plasma configuration approach this extreme limit, the features of the magnetic well (average minimum B), the shear, and their effects on the plasma's MHD stability should deviate from those of standard tokamaks, and the MHD characteristics are expected to change drastically. Since ULART requires a substantially smaller toroidal field current ($I_{tf} \ll I_p$) than conventional tokamaks ($I_{tf} \gg I_p$), it has particularly significant reactor advantages over regular tokamaks. By utilizing the merging spheromak facility with an addition of a slender center TF conductor in the Tokyo University TS-3 device [7], the MHD stability of the ULART configuration can be investigated.

In this paper, we report the recent LART/ULART experimental investigations in three important areas; I. tokamak start-up assist experiments in CDX-U using ECH to minimize the volt-second consumption as well as the induced wall eddy currents, II. investigation of a lower $q(a)$ regime [$q(a) \leq 5$ for $A \approx 1.5$] in CDX-U, and III. investigation both experimentally and theoretically of the MHD characteristics in the ULART regime ($A \approx 1.05 - 1.5$) in TS-3, which has not been previously investigated.

2. Investigation of Tokamak Start-Up and Low $q(a)$ Regimes in CDX-U

2.1 Experimental Set-up

CDX-U is a low-aspect-ratio tokamak facility with $R \approx 35$ cm and $A \geq 1.4$, and with $I_{tf} \leq 240$ kA (steady-state). Presently, an OH power supply with 40 mV-s capability (OH solenoid capability is 150 mV-s) is operational on CDX-U. Four pairs of PF coils are used to control the plasma shape and position. Two 2.45 GHz, 4 kW sources provide initial plasma break-down for the start-up. The device cross-sectional view is shown in Fig. 1. A low base pressure, $P \leq 1-2 \times 10^{-7}$ Torr, is maintained with the combination of cryo-pumping and Ti gettering. The experiment was conducted with hydrogen and helium. Diagnostics include a 2-D scanning microwave interferometer, a poloidal array of magnetic pick-up coils, and a 2-D scannable internal magnetic probe.

2.2 Low-Aspect-Ratio Tokamak Start-up Assist

With ECH, it was possible to initiate low-aspect-ratio tokamak plasmas with a wide range of toroidal field coil current [$I_{tf} = 70$ kA - 160 kA with $R(\text{ECH}) = 16$ cm - 36 cm]. Plasma initiation was also possible with an almost arbitrarily low loop voltage of $V_{\text{loop}} \leq 1$ V, though typically a higher peak voltage of $V_{\text{loop}} \approx 1 - 5$ V was used, depending on the desired current ramp-up rate. A plasma current generating efficiency of 1.7 kA / mV-s was obtained up to $I_p = 53$ kA. Figure 2(a) shows the maximum plasma current obtained thus far in

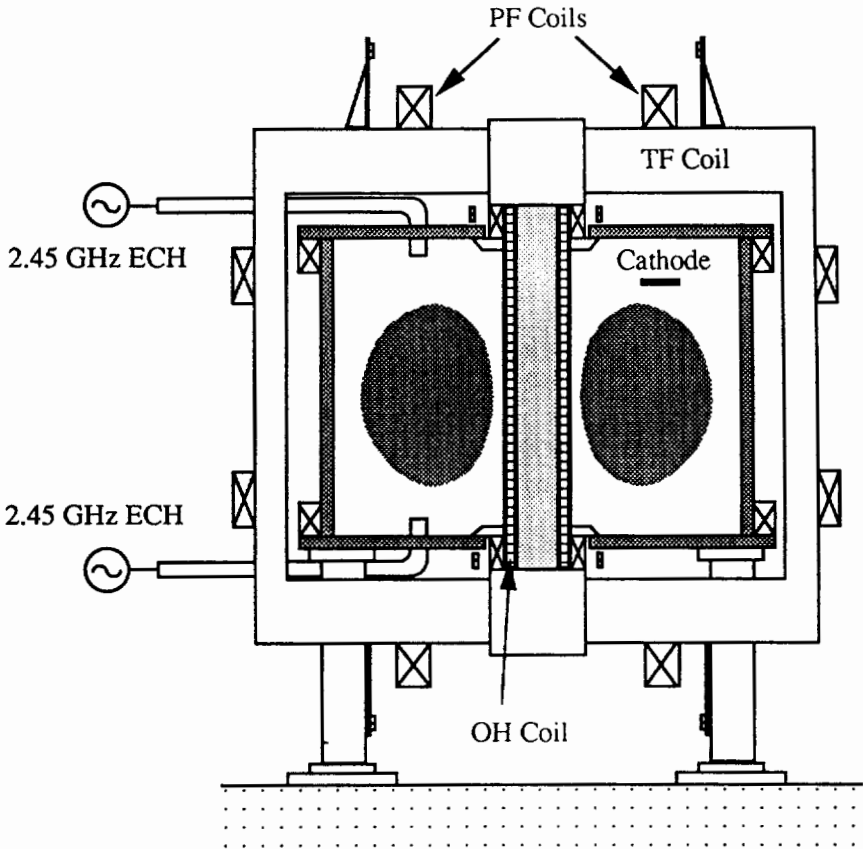


FIG. 1. Schematic of the CDX-U device.

CDX-U ohmic discharges as a function of volt-second expenditure for various discharges. This measure of ohmic heating efficiency can be seen to improve slightly with increasing I_p , suggesting an increasing average temperature with I_p . The maximum current ramp-up rate attained thus far is 10 kA / ms. An Ejima coefficient [8] of 0.4 was routinely obtained. The observed efficiency and the ramp-up rate only dropped by 10% when I_{tf} was reduced by a factor of 2.3 (from $I_{tf} = 160$ kA to 70 kA).

2.3 Lower $q(a)$ Discharge Characteristics

Taking advantage of the relative insensitivity of I_p to the toroidal magnetic field, it was possible to attain $q(a) \leq 5$ tokamak discharges with various toroidal magnetic fields. The maximum plasma current obtained thus far in CDX-U ohmic plasmas, as a function of toroidal field, is shown in Fig. 2(b). Maximum plasma currents at given toroidal magnetic fields seem to be limited by $q(a) \approx 4$ ($q_{cyl} \approx 1$) and $q(0) \approx 1$. Typical plasma parameters for these low $q(a)$, low-aspect-ratio plasmas were: $R = 0.34$ m, $a = 0.22$ m, the line integrated density

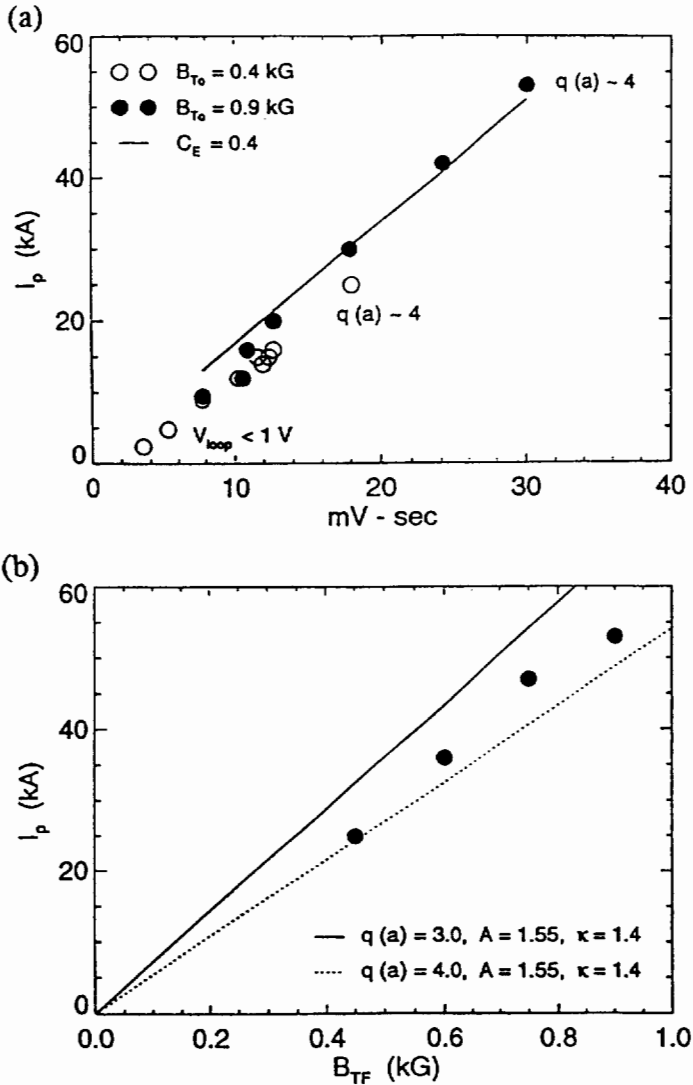


FIG. 2. Ohmic efficiency during CDX-U start-up. (a) I_p versus volt-second expenditure; (b) I_p versus B_{TF} .

$n_e L \approx (4.5 - 10) \times 10^{17} \text{ m}^{-2}$, and estimated $T_{e,av} \leq 100$ eV from neoclassical resistivity with $Z_{eff} = 2$. These parameters indicate that the plasma is already in the low collisionality regime with $\nu^* e \approx 0.1 - 0.3$, where trapped particle effects become important. Maintenance of a 5-10 ms flat-top discharge at $I_p \approx 20$ kA, with an average loop voltage ≈ 1 V also indicates that the plasma has entered a relatively hot, collisionless regime. We typically observe an increase in the

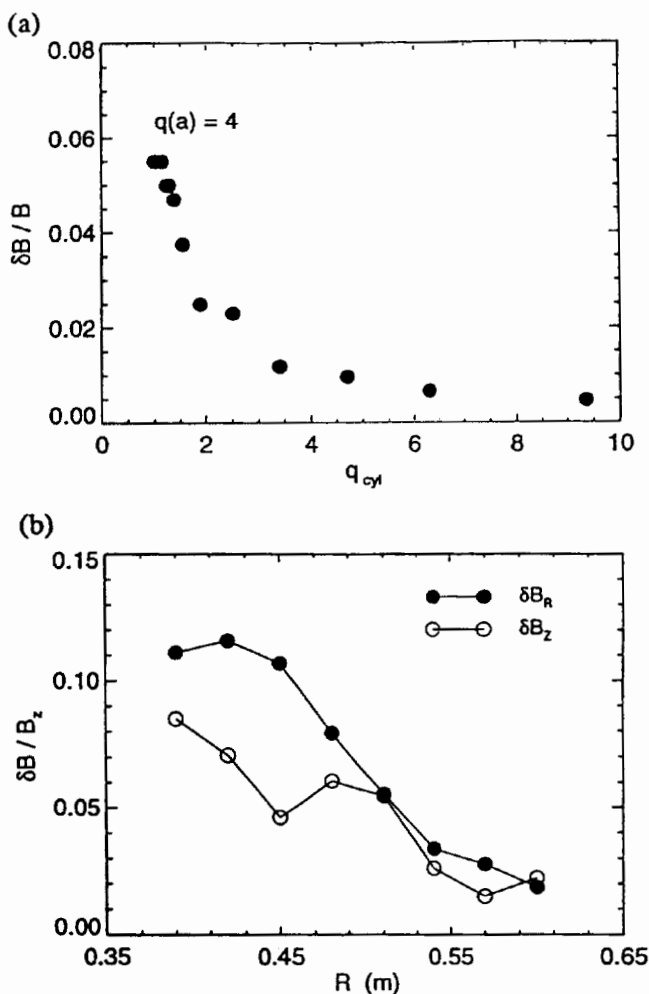


FIG. 3. MHD fluctuations. (a) Poloidal magnetic fluctuation amplitude dependence on $q_{cyl}(a)$. The discharge of $q_{cyl}(a) \approx 1$ is equivalent to that of $q(a) \approx 4$. (b) Radial and vertical magnetic fluctuation variations with major radius at the midplane.

central plasma density and density gradient with the toroidal magnetic field, suggesting an improvement of plasma confinement.

As the $q(a)$ is decreased, however, we observed more frequent abrupt plasma terminations. Most terminations of high $q(a)$ plasmas could be avoided by reducing plasma-limiter interactions with the proper plasma position control. On the other hand, low $q(a)$ plasmas could still terminate even with relatively good position control. As the $q(a)$ is lowered, a strong enhancement of $m=1-2/n=1$ internal MHD modes in the 10-15 kHz range, as shown in Fig. 3(a), was observed. Those modes appear to reduce the current ramp-up rate and, at present, limit the access to even lower $q(a)$ regimes [i.e. $q(a) < 4$ and $q_{cyl}(a) < 1$].

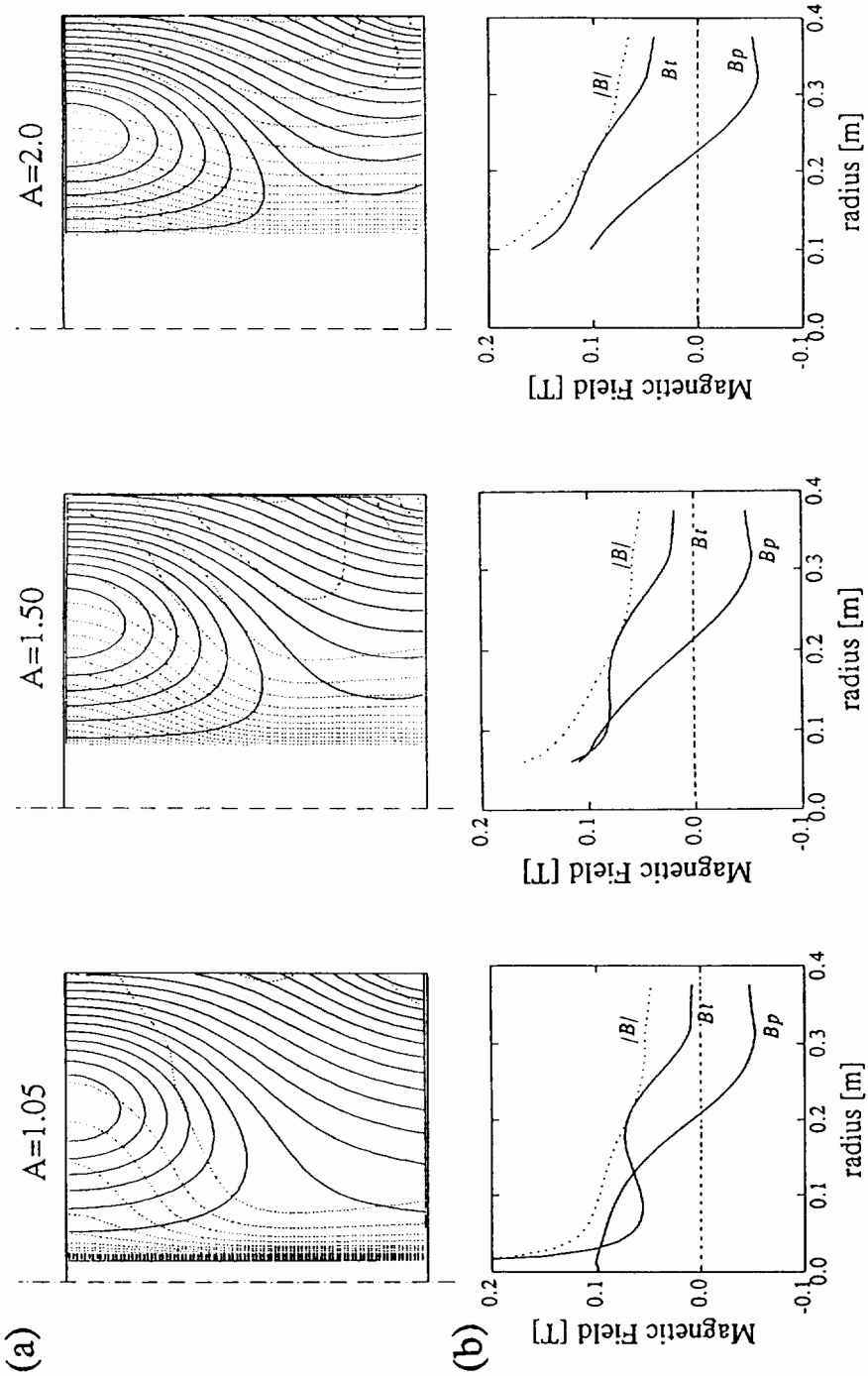


FIG. 4. MHD equilibria of low-aspect-ratio tokamaks for three different aspect ratios, $A = 1.05, 1.5$ and 2.0 . (a) Poloidal flux plots and (b) radial magnetic field profiles of toroidal and poloidal fields (B_t and B_p) and B_{norm} for $q(a) = 3$.

The radial structure of these modes shows a dip in the $\delta B_Z/B_Z$ signal but not in the $\delta B_R/B_Z$ signal as shown in Fig. 3(b), which suggests the possible existence of large magnetic islands at the low field side. As the central safety factor, $q(0)$ goes down to less than one, these islands can couple with $m=1/n=1$ sawteeth and terminate the plasma abruptly. The $q(0)$ of maximum plasma current discharges for various toroidal magnetic fields were estimated to be near one, which supports the above conjecture. Detailed studies of these modes are ongoing. Possible stabilization schemes such as DC-helicity injection to flatten the current profile are also being considered.

The behavior of MHD and kinetic fluctuation activities (using various probes and a tangential CO₂ phase-contrast-imaging system) and related confinement as a function of the plasma aspect-ratio, $q(a)$, and plasma collisionality are presently under study.

3. Investigations of ULART Plasmas in the TS-3 Device

3.1 Characteristics of the ULART Configuration

MHD equilibrium calculations show that the ULART plasmas with edge safety factor of $q(a) > 3$ (q is the inverse of the rotational transform of field lines) are characterized by high maximum toroidal beta, low poloidal beta, high natural elongation, strong paramagnetism, and a large ratio of plasma current to toroidal-field-coil current. Figure 4 presents poloidal flux contours and poloidal magnetic field profiles of a $q(a)=3$ tokamak for three different aspect ratios of $A=1.05, 1.5$ and 2.0 . The paramagnetism is seen to increase as A decreases. In the low-aspect-ratio limit, the field line pitch resembles that of a spheromak in the outer radial edge of a toroidal plasma, but it has a large toroidal field component in the inner radial edge, just like in a tokamak. The global stability of the ULART is determined by the magnetic well depth (not always present) and the shear of the configuration. One of the most important global modes is the $m=1/n=1$ tilt/shift mode.

Since the ULART requires a very small axial coil current to generate the necessary toroidal field for a tokamak confinement configuration, it has important reactor advantages over regular tokamaks. We have calculated required axial coil current for typical ULART configurations using (1) simplified analytical calculation and (2) computer equilibrium code calculation based on the Grad-Shafranov equation. Our analytical calculation is based on a simplified model in which q is predominantly determined by the field line pitch in the inner toroidal edge of the ULART [9]:

$$B_t = \mu_0 I_{tf} / 2 \pi R_{tf}, \quad (1a)$$

$$B_p \approx \mu_0 I_p / 2 L_p, \quad (1b)$$

$$q(a) \approx (B_t L_p) / (B_p 2\pi R_{tf}), \quad (1c)$$

where L_p and R_{tf} are vertical length of the plasma and radius of the inner toroidal coil. By combining equations (1a), (1b), and (1c), we obtain

$$I_{tf} / I_p \approx 2 q(a) (\pi R_{tf} / L_p)^2. \quad (2)$$

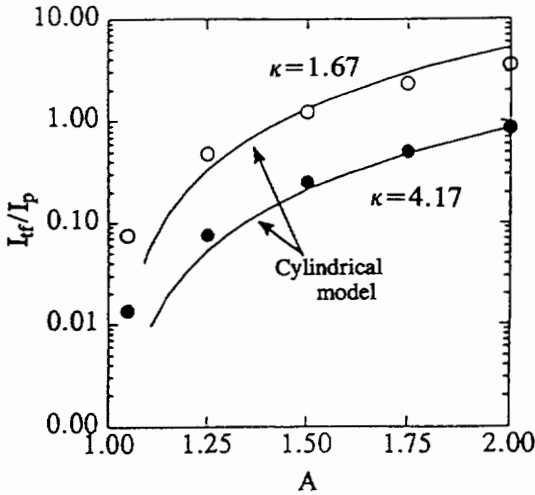


FIG. 5. Required toroidal coil current (I_{tf}/I_p) versus aspect ratio A for ULART equilibrium with $q(a) = 3$ and for $\kappa = 1.67$ and 4.17 .

With a relationship between aspect ratio A and the plasma's major radius R_p ($= a + R_{tf}$) and minor radius, a :

$$A = (a + R_{tf}) / a = 1 + R_{tf} / a,$$

we obtain an analytical approximation for toroidal coil current,

$$I_{tf} / I_p = 2 q(a) (\pi a / L_p)^2 (A - 1)^2. \quad (3)$$

Figure 5 presents the ratios of (total) toroidal coil current (I_{tf} ; Ampere-turns) over plasma current (I_p) versus various aspect ratios ranging from 1.05 - 2.0 for $q(a)=3$ and $\kappa=L_p/2a = 1.67$ or 4.17 . The curves shown in Fig. 5 are from Eq.(3) and agree well with more exact calculations based on the Grad-Shafranov equation. One notices that ULART requires substantially smaller toroidal field current ($I_{tf} \ll I_p$) than conventional tokamaks ($I_{tf} \gg I_p$), and that the ratio (I_{tf} / I_p) can be as small as 0.1 for an ultra low aspect ratio tokamak with $A=1.1$ and $q(a)=3$.

3.2 Experimental Study of the Global Stability

It has been known that the spheromak's tilt mode can be stabilized either by passive stabilizers and/or figure 8 coils [10], or by an external toroidal field, but not by a thin passive center conductor (because of ineffectiveness of small image currents). The question arises of what amount of external toroidal field is necessary to stabilize the $n=1$ tilt mode. By introducing a slender current-carrying conductor assembly ($R_{tf} \geq 1$ cm) through the geometric center axis of the TS-3 device, we have generated ULART configurations with extremely low

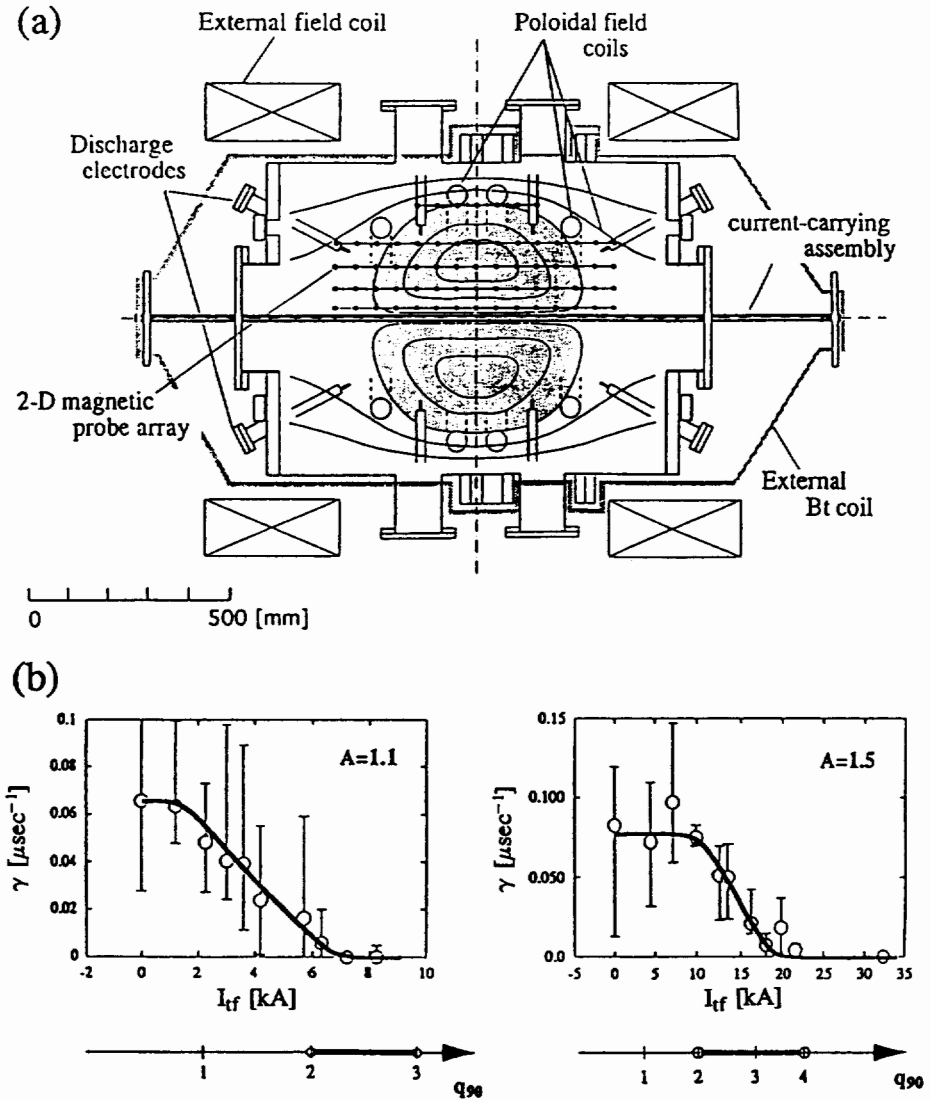


FIG. 6. (a) Schematic of the TS-3 device for ULART experiments. (b) Growth rate of the $n = 1$ toroidal mode versus I_{tf} in the TS-3 ULART regime with $A = 1.1$ ($I_p \approx 30$ kA) and $A = 1.5$ ($I_p \approx 20$ kA), where q is defined at $\Psi/\Psi_a = 90\%$.

aspect ratios of 1.05-1.5. In this extreme limit we investigate the transition of the spheromak ($q(a) = 0$, $I_{tf}=0$) to a ULART plasma ($q(a) = 2-20$). The attainable plasma current is 30 - 40 kA with variable toroidal field of 0-2 kG for $R_p=18$ cm, $a \leq 16$ cm. The evolution of the current and magnetic profile [$q(R)$, $B(R)$, $\psi(R)$] is monitored by an array of magnetic probes immersed in the plasma. Figure 6(a) presents the basic geometry of the TS-3 device[11].

A significant observation is the effectiveness of the central toroidal current against tilt and kink modes. An important question is at what I_{tf} the plasma becomes stable by suppressing the $n=1$ tilt/kink mode. It is observed that a small axial current ($I_{tf} \ll I_p$) in the center conductor can significantly improve the overall stability of the plasmas. Figure 6(b) depicts the $n=1$ component of the plasma displacement due to tilt/shift or kink modes versus time for different toroidal coil currents at the center conductor. It is observed that the growth rate of the $n=1$ mode decreases drastically as toroidal coil current is raised or q is increased. The threshold value of I_{tf} for $n=1$ global stability decreases substantially from about 20 kA to 6.0 kA as A is reduced from 1.5 to 1.1. These threshold cases correspond to $q_{90} = 2 - 4$ at the plasma edge of $\psi/\psi_a = 0.90$. A simple MHD theory predicts $\langle B_t \rangle \geq \langle B_p \rangle$ for external tilt stability for a large aspect ratio limit, which is easily satisfied in conventional tokamak configurations. If we apply the same criterion to the ULART, the threshold value for tilt mode stability would be $q_{cyl}(a) = a/R_p \sim 1$ (where $q_{cyl}(a)$ denotes cylindrical q value) or $I_{tf} \geq I_p$. However, our experiment has demonstrated that notably smaller I_{tf} is required for $n=1$ tilt/shift global stability. In Fig. 6 the stable regime is shown by $I_{tf} \geq 0.2 I_p$ for $A=1.1$. The present result from the ULART experiment on TS-3 is consistent with the CDX-U result in which a significant enhancement of $m=1-2/n=1$ internal MHD modes is observed as the $q(a)$ is decreased as shown in Fig. 3(a). Here, we expect a coupling of low- n internal modes with external modes. A further extensive investigation with the aid of MHD numerical stability codes will clarify this important issue and reveal many more unique MHD characteristics of the ULART configuration.

ACKNOWLEDGMENT

This work was supported by USDOE contract No. DE-AC02-76-CHO-3073 and Mombusho of Japan.

REFERENCES

- [1] PENG, Y.-K.M., GALAMBOS, J.D., SHIPE, P.C., *Fusion Technol.* **21** (1992) 1729.
- [2] SYKES, A., et al., *Plasma Phys. Control. Fusion* **35** (1993) 1051.
- [3] ONO, M., et al., in *Plasma Physics and Controlled Nuclear Fusion Research 1992* (Proc. 14th Int. Conf. Würzburg, 1992), Vol. 1, IAEA, Vienna (1993) 693.
- [4] ROBINSON, J., et al., *Bull. Am. Phys. Soc.* **38** (1993) 2005.
- [5] PENG, Y.-K.M., STRICKLER, D.J., *Nucl. Fusion* **26** (1986) 769.
- [6] REWOLDT, G., TANG, W.M., in *Proc. Int. Sherwood Theory Mtg San Antonio, TX, 1989*, Paper 1C26.
- [7] ONO, Y., et al., *Phys. Fluids B* **5** (1993) 3691.
- [8] EJIMA, S., et al., *Nucl. Fusion* **22** (1982) 1313.
- [9] KATSURAI, M., et al., paper presented at IEE Japan Plasma Workshop, EP-94-53, 1994.
- [10] YAMADA, M., et al., in *Plasma Physics and Controlled Nuclear Fusion Research 1984* (Proc. 10th Int. Conf. London, 1984), Vol. 2, IAEA, Vienna (1985) 535.
- [11] MORITA, A., et al., *Bull. Am. Phys. Soc.* **38** (1993) 2008.